Modeling detector performance in digital mammography using the linear cascaded systems approach

V. Spyropoulou[a,b], N. Kalivas[a,b], A. Gaitanis[a,b], C. Michail[a,b], G. Panayiotakis[b], I. Kandarakis[a*]

[a] *Department Medical Instruments Technology, Technological Educational Institution of Athens, Ag. Spyridonos, Aigaleo, 122 10 Athens, Greece*
[b] *Department of of Medical Physics, Medical School, University of Patras, 265 00 Patras, Greece*
* Corresponding author: kandarakis@teiath.gr

Abstract

Digital x-ray mammography is a modern method for the early detection of breast cancer. The quality of a mammography image depends on various factors, the detector structure and performance being of primary importance. The aim of this work was to develop an analytical model simulating the imaging performance of a new commercially available digital mammography detector. This was achieved within the framework of the linear cascaded systems (LCS) theory. System analysis has allowed the estimation of important image quality metrics such as the Modulation Transfer Function (MTF), the Noise Power Spectrum (NPS), the Detective Quantum Efficiency (DQE) and the Signal to Noise Ratio (SNR). The detector was an indirect detection system consisting of a large area, 100μm thick, CsI:TI scintillator coupled to an active matrix array of amorphous silicon (a-Si:H) photodiodes combined with thin film transistors (TFT). Pixel size was 100μm, while the active pixel dimension was 70μm. MTF and DQE data were calculated for air kerma conditions of 25, 53, 67 μGy using a 28 kVp Mo-Mo x-ray spectrum. In addition, the scintillator thickness was changed in order to find the optimum material characteristics. The theoretical results were compared with published experimental data. The deviation between the theoretical and experimental MTF curves was less than 4%, while the DQE differences were found at an acceptable level.

Keywords: *Digital mammography; Image quality;Linear cascaded systems theory; Indirect detectors;*

1. Introduction

Digital x-ray mammography is a modern method for the early detection of breast cancer. In mammography, detector optimization is of primary concern due to limitations originating from trade offs between detail visualization and quantum detection efficiency.

The aim of the present work was to apply a theoretical model for the calculation of image quality parameters such as the Modulation Transfer Function (MTF) and the Detective Quantum Efficiency (DQE) and Signal to Noise Ratio (SNR) using the

linear cascaded systems theory, based on the theoretical framework introduced by Cunningham (1998) [1]. This theory has been previously applied by Siewerdsen et al (1996) [2], El-Mohri et al (2001) [3] and Jee et al (2003) [4] to study x-ray digital radiography and digital mammography detectors. In these studies, however, the properties of intrinsic energy conversion and optical properties of the scintillator (type of scintillator, surface density, intrinsic conversion efficiency, optical photons propagation in the material) were not taken into account systematically. In the present work a detailed account of the conversion and optical properties of the scintillator was incorporated in the model framework. The detector studied consisted of a CsI:TI scintillator deposited on an a-Si:H active matrix photodiode-TFT array. Model results were found in good agreement with experimental data published in the literature [5].

2. Materials and methods

2.1. System Description

In this study a theoretical model was developed in a Matlab platform to describe the operation of a flat panel detector used in digital mammography. The detector was considered to be an indirect detector, particularly CsI: TI with a: Si-H photodetectors. The thickness of CsI: TI was 100μm and the active pixel dimension was 70μm [4, 5].

2.2. Cascaded systems model

A theoretical model, based on the linear cascaded systems theory [1-7], was applied το simulate a digital imager configuration. The latter was represented as a series of cascaded signal amplification and/or signal blurring stages. Each stage represents a physical wide sense stationary (WSS) process [1] that governs the transfer of signal and noise from the input to the output of the cascaded stages [2]. The signal detection is assumed to be described by nine stages as shown in fig.1
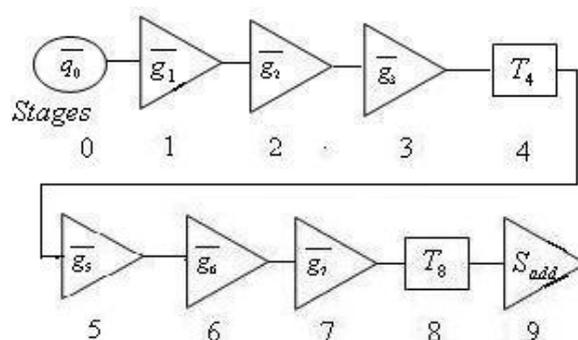
Figure 1. Shows the block diagram of various stages involved in the formation of x-ray imagers in digital mammography.

The signal detection process was assumed to consist of nine stages:
  Stage 0 represents the input of the system, i.e. the x-ray quanta incident on the detector *(q_0)*. *Stage 1* represents the fraction of x-ray quanta that interact with the CsI:TI scintillator. This stage was represented by a binomial selection process with a gain *g_1*. *Stage 2* represents the x-ray quanta converted to optical quanta inside the scintillator. This stage is a signal amplification (gain) process *(g_2)*, described by a Poisson distribution. *Stage 3* represents the optical quanta escaping the scintillator,

and is described by a gain process *(g₃)*, with a binomial distribution. *Stage 4* represents the multiple scattering (spreading) of the optical quanta within the scintillator. Such optical scattering create a stochastic blur process due to modifications in the spatial distribution of optical quanta described by the MTF of this stage *(T₄)*. *Stage 5* represents the optical photons coming out of the CsI:TI, which are finally captured by the amorphous silicon (a:Si) photodiodes. This is a gain process *(g₅)*, described by a binomial distribution. The fraction of optical quanta finally captured by the photodetector depends on the spectral compatibility between the emitted light spectrum and the sensitivity of the photodetector (matching factor). *Stage 6* stands for the optical photons that interact with the amorphous silicon producing electron-hole pairs (e-h). This is a gain process *(g₆)*, described by a binomial distribution. Stage 7 stands for the propagation of electron-hole pairs to the photodetector output. This stage is described by a gain process *(g₇)* and a binomial distribution. Stage 8 is a deterministic blur process that is characterized by the MTF *(T₈)* of the photodiode before sampling. It depends on the photodiode dimensions. Finally, the noise of the imager's electronic acquisition system is added as a separate term *(S$_{acq}$)* to the imaging chain. In the present study we have considered S_{acq} =1000e^-, in accordance with a previous publication [4].

Furthermore some assumptions, for the stages mentioned above, have been taken into consideration. These are: a) in previous studies [11,12] it has been shown that the MTF of a structured phosphor, like the needle-like shaped crystals of CsI, is comparable to that of a powder phosphor screen of half the thickness [8]. Thus, the analytical models established for powder phosphors [11,12] can be used for structured phosphors provided the effective thickness is modified appropriately [8], b)a proportion of 1:1 between captured optical photons and generated e-h pairs was assumed [2], c) spreading of electron-hole pairs was assumed to be negligible [2].

2.3. *Modulation Transfer Function (MTF)*

MTF, expressing signal transfer through blurring system stages [9] was expressed in terms of the individual MTFs of the system.

$$MTF_{system} = T_4(u) \times T_8(u)$$

(1)

Where T_4 is the *MTF* of CsI:TI scintillator and T_8 is the *MTF* of the photodiode array.

2.4. *Detective Quantum Efficiency (DQE)*

By definition, *DQE* compares the *SNR* (signal-to-noise ratio) at the detector output (digital signal) with that at the detector input (X-ray flux at the entrance window) as a function of spatial frequency *u*. In the present study *DQE* was expressed by the relation [9]:

$$DQE(u) = \frac{\overline{q_8^2} MTF^2(u)}{\Phi NPS(u)}$$

(2)

Where q_8 is the mean signal value at the detector output, *NPS(u)* is the total Noise Power Spectrum that provides an estimation of the spatial frequency dependence of the pixel-to-pixel fluctuations present in the image of the system that was derived from all stages of the detector and Φ is the incident x-ray fluence.

2.5. Signal to Noise Ratio (SNR)

SNR is also used as an indicator of the existence of a circular tumor of various shapes, against a homogeneous noisy background, which was considered to be a breast. The *SNR* can be written as [6]:

$$SNR = \frac{\overline{S_1} - \overline{S_2}}{\left(\sigma^2(S_1) + \sigma^2(S_2)\right)^{1/2}} \tag{3}$$

Where $\overline{S_1}$ is the mean signal value of the breast area and $\overline{S_2}$ is the mean signal value of the tumor area. The distribution of $\overline{S_1} - \overline{S_2}$ is assumed to be Gaussian [6]. $\sigma^2(S)$ is the corresponding variances [10] :

$$\sigma^2 = \sum_0^u NPS(u) \tag{4}$$

3. Results and discussions

Figure 2 shows a comparison between the calculated pre-sampling MTF and those taken from the literature. It is shown that the difference between those two curves is negligible. In particular, the deviation between the theoretical and the experimental results are less than 4%.
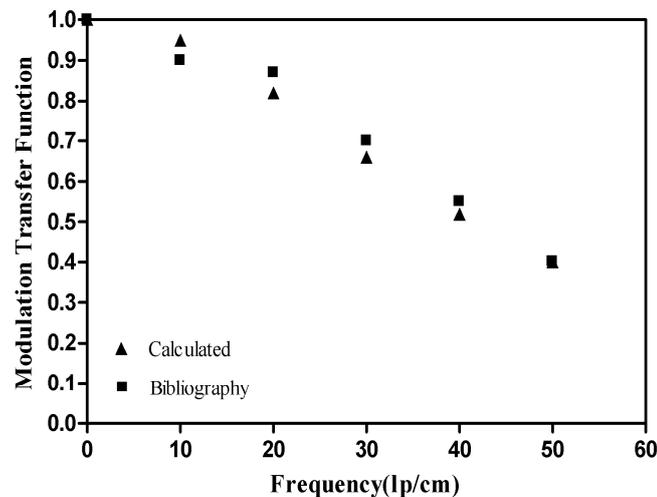
Figure 2. Pre-sampling MTF calculated by our model versus bibliographic data for 25μGy air kerma of Mo/Mo.

Figure 3 shows the pre-sampling MTF for three (50, 100 and 200 μm) different CsI:TI scintillator thickness.

It is shown that MTF decreases with increasing thickness. Best MTF values were found at 50μm.
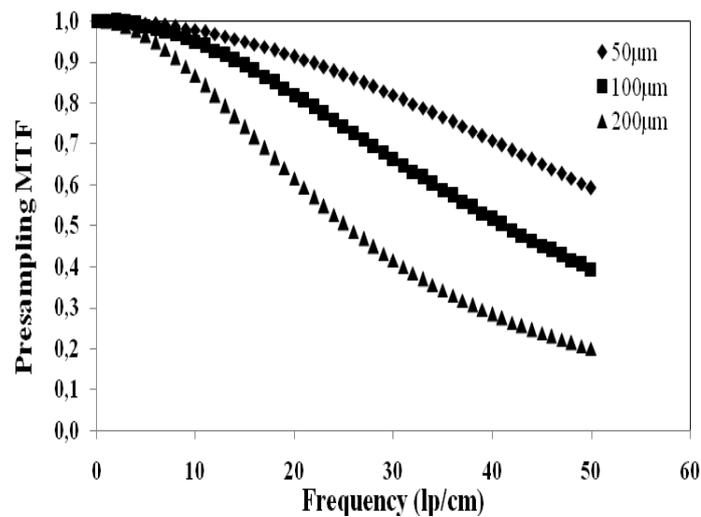
Figure 3. Pre-sampling MTF, Mo/Mo, 28kVp, 67μGy air kerma and various thicknesses of CsI:TI.

Figure 4 shows the calculated DQE for 67μGy air kerma, Mo/Mo spectrum and different thickness of scintillator. The CsI:TI thickness values were the same as in figure 3.
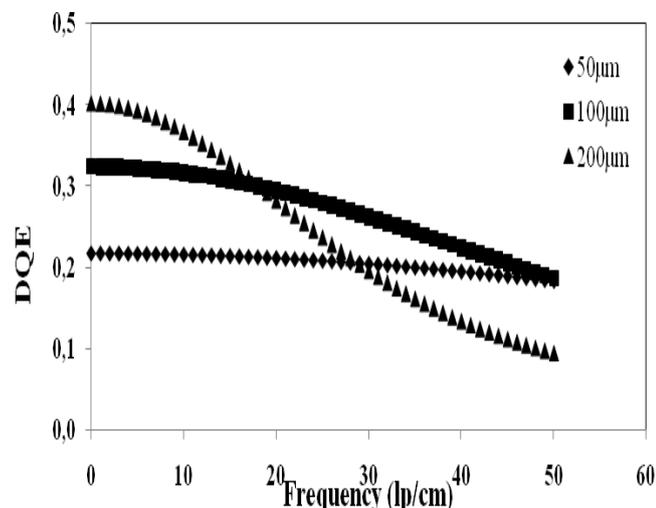
Figure 4: DQE Mo-Mo spectra, 28kVp, 67μGy air kerma and various thicknesses of CsI:TI.

At low frequencies, from 0 up to 12 lp/cm, DQE appears to be better for the 200μm scintillator thickness. However in the range of frequencies from 30 up to 50 lp/cm, DQE drops rapidly showing lower values with respect to the other two scintillator thickness. Furthermore, the thickness of 100 μm showed better values for DQE than 50 μm at low frequencies and at 40 lp/cm appears to be the same.

The model was also used for the *SNR* calculation for various air kerma values (5 and 10 *μGy*) and different tumor diameters at 28kVp tube voltage. It was found that

SNR increases with increasing air kerma. Particularly, it was found that for 0.1mm tumor thickness and 5 *μGy*, *SNR* was 0.02 while for 10 *μGy* SNR was found 9.03.

4. Conclusion

A theoretical model was developed to simulate the operation of a detector used in digital mammography. The results of the model developed were found to be in an acceptable agreement with previously published experimental data. Particularly, the results of the theoretical and the experimental results of the pre-sampling *MTF* were found less than 4%. Furthermore, the 100μm thick CsI:TI scintillator was found better than the corresponding 50 and 200μm thick scintillators due to its higher MTF and DQE values.

References

[1] Cunningham I.A. (1998), "Linear-Systems modeling of parallel cascaded stochastic processes: The NPS of radiographic screens with reabsorption of characteristic X radiation", *Physics of Medical Imaging, Proc. SPIE 3336*, pp.220-230.

[2] Siewerdsen J.H., Antonuk L.E., El-Mohri Y., Yorkston J., Huang W., Boudry J.M., Cunningham I.A. (1996), "Empirical and theoretical investigation of the noise performance of indirect detection, active matrix flat- panel imagers (AMFPIs) for diagnostic radiology", *Med. Phys., Vol.24 (1),* pp.71-89.

[3] El-Mohri Youcef, Jee Kyung-Wook, Antonuk E.Larry, Maolinbay Manat, Zhao Qihua (2001), "Determination of the detective quantum efficiency of a prototype, megavoltage indirect detection, active matrix flat-panel imager", *Med. Phys., Vol.28(12)*, pp.2538-2550.

[4] Jee Kyung-Wook, Antonuk E. Larry, El-Mohri Youcef, Zhao Qihua, "System performance of a prototype flat-panel imager operated under mammographic conditions", *Med. Phys., Vol. 30(7),* pp.1874- 1890.

[5] Rivetti Stefano, Lanconelli Nico, Campanini Renato, Bertolini Marco, Borasi Gianni, Nitrosi Andrea, Danielli Claudio, Angelini Lidia and Maggi Stefania (2006), "Comparison of different commercial FFDM units by means of physical characterization and contrast-detail analysis", *Med. Phys.Vol.33(11),*pp.4198-4209.

[6] Markku J. Tapiovaara and Robert F. Wagner, "SNR and DQE analysis of droad spectrum x-ray imaging", *Phys. Med. Biol., Vol. 30(6)*, 1985, 519-529

[7] Cunningham I.A. (2000) 'Applied Linear-Systems Theory' in: Handbook of Medical Imaging, Vol. 1, Physics and Psychophysics, edited by Beutel J., Kundel H.L., Van Metter R.L., SPIE, Bellingha.

[8] W. Zhao, G. Ristic, J.A. Rowlands (2004), "X-ray imaging performance of structured cesium iodide scintillators" Med. Phys.31 (9), pp.2594- 2605.

[9] Martin Spahn (2005), "Flat detectors and their clinical applications", *Eur.Radiol. Vol.15*, pp.1934-1947.

[10] I.A. Cunningham and R. Shaw (1999), "Signal-to-noise optimization of medical imaging systems", *J.Opt.Soc,Am.A, Vol.16,* pp 621-632.

[11] N. Kalivas, L. Costaridou, I. Kandarakis, D. Cavouras, C.D. Nomicos, G. Panayiotakis (2002), "Modeling quantum and structure noise of phosphors used

in medical X-ray imaging detectors", *Nuclear Instruments and Methods in Physics Research A 490*, pp.614–629.

[12] D. Cavouras, I. Kandarakis, D. Nikolopoulos, I. Kalatzis, G. Kagadis, N. Kalivas, A. Episkopakis, D. Linardatos, M. Roussou, E. Nirgianaki, D. Margetis, I. Valais, I. Sianoudis, K. Kourkoutas, N. Dimitropoulos, A Louizi, C. Nomikos, G. Panayiotakis (2005), "Light emission efficiency and imaging performance of $Y_3Al5O12$:Ce(YAG:Ce) powder screens under diagnostic radiology conditions", *Appl. Phys. B80*,pp. 923-933.